

# A new method for gaining insight into the chemistry of drying mineral surfaces using ATR-FTIR

Catherine E. Dowding<sup>a,\*</sup>, Michael J. Borda<sup>b</sup>, Martin V. Fey<sup>a</sup>, Donald L. Sparks<sup>b</sup>

<sup>a</sup> *Department of Soil Science, University of Stellenbosch, South Africa*

<sup>b</sup> *Department of Plant and Soil Sciences, University of Delaware, USA*

Received 22 December 2004; accepted 21 May 2005

Available online 14 July 2005

## Abstract

Although it is understood that the chemical environment at a drying surface is likely to be quite different from that at a fully hydrated surface, the difficulty of quantitative measurement has meant that this potentially crucial aspect of surface chemistry has gone largely overlooked. As a result, most of our understanding comes from measurement before and after drying, with a gray region of speculation in between. An interesting natural example is the paradoxical reduction of Mn oxides in moist soils as they dry, because drying is usually considered an oxidative process. This phenomenon indicates that important chemical changes are occurring during drying and an approach is needed to probe the chemistry of drying surfaces. Here we show the suitability of attenuated total reflectance Fourier transform infrared (ATR-FTIR) spectroscopy for real-time, in situ investigation of the drying solid–water interface, using the change in surface pH as an example. This was achieved by adsorbing thymol blue pH indicator ( $pK_a = 1.65$ ) onto a natural Mn-rich clay and observing the real-time pH change, which dropped from pH 5 to below pH 1.65 with the removal of free water from the surface.

© 2005 Elsevier Inc. All rights reserved.

**Keywords:** Thymol blue; Surface acidity; Drying; ATR-FTIR

## 1. Introduction

Wetting and drying cycles are an everyday event in terrestrial environments. Very little is known, however, about the chemical changes that occur on drying solid–water interfaces. It has been suggested that drying a clay surface is an acidifying process due to the dissociation of the last few monolayers of water surrounding adjacent polarizing cations [1]. This process, however, has been hard to quantify and little is known about the repercussions of this and other drying-induced changes. Drying soils is known to increase their fertility [2], cause substantial Mn release, and change their redox properties [3–5]. It has been speculated that H-bonding and therefore the stability of humic compounds is affected by drying [6]. Surface charge and metal

bonding of colloidal oxides change with hydration state [7] and the chemical conditions associated with wetting and drying are known to be fundamental to atmospheric corrosion of iron [8]. These examples from varying fields of research highlight the need for a real-time, in situ probe to elucidate chemical changes that occur during the removal of water from a drying surface.

Vibration spectroscopy in the infrared region is particularly sensitive to the presence of water and is therefore useful for probing the degree of surface dehydration. The ATR-FTIR technique allows chemical changes associated with water removal from the mineral–water interface to be studied in situ, under ambient conditions. It is sensitive to species adsorbed at the solid–water interface and can be used to analyze surface reactivity promoted by the drying process.

The present study, involving the examination of colloid extracted from a manganese-rich soil, represents the first spectroscopic observation, to the authors' knowledge, of

\* Corresponding author.

E-mail address: [cathydowding@yahoo.co.uk](mailto:cathydowding@yahoo.co.uk) (C.E. Dowding).

a pH change on colloid surfaces collected in real time. This study demonstrates ATR-FTIR as a novel, straightforward technique for investigating reactions at drying interfaces.

## 2. Materials and methods

A clay separate was extracted from the subsoil of a highly weathered, manganese-rich soil from the Graskop district in the Mpumalanga Province of South Africa. This porous, friable black soil contains more than 50% clay, 0.25% carbon, and 7% manganese. Clay mineral composition is dominated by lithiophorite ((Al,Li)MnO<sub>2</sub>(OH)<sub>2</sub>), with accessory amounts of gibbsite (Al(OH)<sub>3</sub>), goethite ( $\alpha$ -FeOOH), hematite (Fe<sub>2</sub>O<sub>3</sub>), maghemite ( $\gamma$ -Fe<sub>2</sub>O<sub>3</sub>), and kaolinite (Al<sub>2</sub>Si<sub>2</sub>O<sub>5</sub>(OH)<sub>4</sub>). The pzc of the soil, as determined potentiometrically, is 5.5.

The clay fraction was separated from the bulk soil by shaking and sedimentation after lowering the aqueous suspension pH to 4 with HCl. After the suspension was restored to pH 5 with NaOH the dispersed clay was flocculated using MgSO<sub>4</sub> and washed several times with ultrapure deionized (DI) water. The clay was resuspended and diluted to a concentration of approximately 30 mg/L in a 30:70 ethanol:water solution. A thin clay film was air-dried on a germanium (Ge) internal reflection element (IRE) for examination by ATR-FTIR spectroscopy using a Thermo Electron Nexus 670 spectrometer fitted with a liquid-N<sub>2</sub> cooled MCT-A detector and a Horizontal ATR flow-through assembly (PIKE Technology). The Ge IRE was chosen for its greater acid stability as compared with the more commonly used ZnSe IRE.

The dry clay film was rehydrated in the flow cell with DI water and a background scan of the fully hydrated clay was collected. All subsequent scans were ratioed against the hydrated-clay background, allowing peak intensity due to water loss and the sorbed indicator to be observed. A pH 5.6 solution of thymol blue (C<sub>27</sub>H<sub>30</sub>O<sub>5</sub>S) was injected into the flow cell to give a final concentration in contact with the clay of  $5 \times 10^{-5}$  M. This concentration is well below the infrared detection limit for aqueous species on the IRE used in ATR-FTIR [9,10], permitting any thymol blue detected to be considered surface-bound. The clay film, with sorbed indicator, was allowed to dry gradually at room temperature during a dry-air purge of the spectrometer. During the entire drying period, spectra were collected every minute using 64 co-added scans at 4 cm<sup>-1</sup> resolution.

Standard spectra of 25 mM solutions of thymol blue at pH 5.6 and 1.2 (deprotonated and protonated, respectively) were collected on a clean Ge crystal. A set of control spectra was collected for thymol blue that had been allowed to dry from a  $5 \times 10^{-5}$  M solution on the clean Ge crystal. The only observable change in the control spectra was a concentration-dependent increase in peak intensity due to evaporation of water and a consequent increase in the ac-

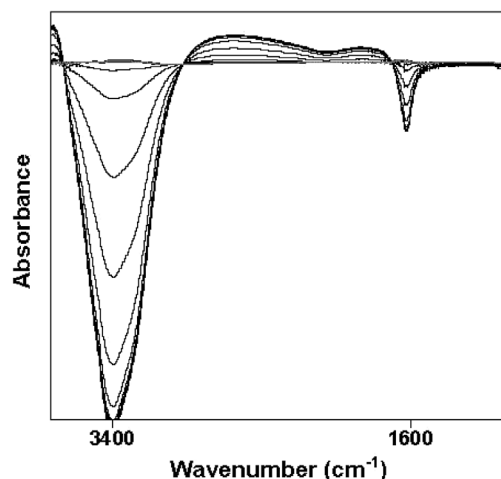


Fig. 1. Selected spectra showing progressive water removal as a hydrated clay film was evaporated over an 8-h period on a Ge crystal. The negative absorption band at 1600 cm<sup>-1</sup> signifies the loss of water relative to the fully hydrated clay background. The eventual superimposition of spectra indicates removal of free water from the surface.

tivity of solution species. No new peaks or shifts in peak positions were observed in the control experiment.

## 3. Results and discussion

The spectra of the drying clay film are shown in Fig. 1. Two water bands are present, one band in the region 3200–3500 cm<sup>-1</sup> and a second at approximately 1600 cm<sup>-1</sup>. The broad spectral intensity in the region 3200–3500 cm<sup>-1</sup> is due to the  $\nu_1$  symmetric stretching mode for water, along with OH stretching modes from surface functional groups. The peak at approximately 1600 cm<sup>-1</sup> is due to the  $\nu_2$  bending mode of water. This bending mode is therefore a much more sensitive indicator of surface dehydration because there are no vibrational band overlaps due to surface functional groups. The intensity of the 1600 cm<sup>-1</sup> peak became increasingly more negative with drying, until successive spectra in this region superimposed, indicating that the surface had come to equilibrium with the humidity (1 ppm) of the dry-air purge in the reaction chamber. A possible limitation of this technique is the loss of information in the 3400- and 1600-cm<sup>-1</sup> regions due to the large negative absorption bands. This requires the sorbate, in this case the indicator, to have active functional groups outside the large water bands. The sulfonate indicators are particularly well suited for this purpose due to the absorbance of sulfonate in the region 1180–1240 cm<sup>-1</sup>.

Spectra for the protonated and deprotonated thymol blue standard solutions are shown in Fig. 2. The region between 1120 and 1380 cm<sup>-1</sup> shows the largest spectral difference between the protonated and deprotonated forms of the indicator, which was interpreted as the protonation/deprotonation of the sulfonate (SO<sub>3</sub><sup>-</sup>) group (1120 and 1280 cm<sup>-1</sup>) and the formation of a phenyl group (1340–

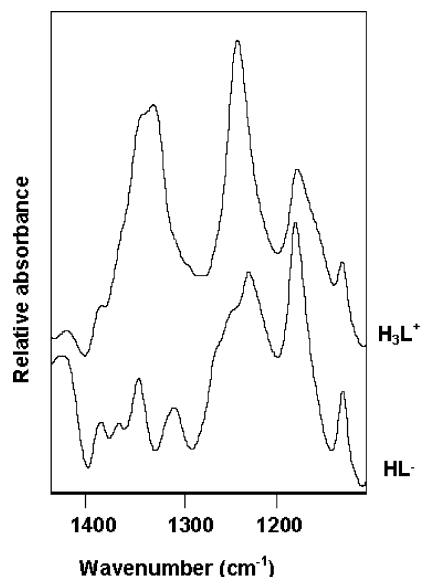


Fig. 2. IR spectra of protonated (pH 1.2) and deprotonated (pH 5.6) thymol blue standards using 0.025 M solutions equilibrated on a clean Ge crystal. HL<sup>-</sup> represents the dominant species of the indicator at pH 5, and H<sub>3</sub>L<sup>+</sup> represents the fully protonated indicator, which would be the dominant species at pH 1.2.

1370 cm<sup>-1</sup>). Thymol blue has been described as having three acid–base equilibria [11]. In this model, protonation of the blue deprotonated indicator (L<sup>2-</sup>) leads to the yellow (HL<sup>-</sup>) species (p*K<sub>a</sub>* 8.9). Protonation of the sulfonate group results in the formation of the uncharged, yellow (H<sub>2</sub>L) species (p*K<sub>a</sub>* 4.1 [12]). The change from yellow to red (H<sub>3</sub>L<sup>+</sup>) involves the formation of a phenyl group (p*K<sub>a</sub>* 1.65). Both the protonation of the sulfonate group and the formation of the phenyl group can be seen in the acidified indicator.

Fig. 3 shows a time series of spectra during the drying of thymol-blue-treated clay. More than 1000 scans were collected over an 8-h period; however, for clarity only a selection of the spectra have been included. Two distinctly different spectral patterns are apparent: those representing the hydrated surface (upper group), which resemble the spectrum of the deprotonated indicator, and those representing the dry surface (lower group), which resemble the spectrum of the protonated indicator (Fig. 2). The first shift in the region 1240–1185 cm<sup>-1</sup> is linked to the first negative water band (Fig. 1), indicating that a change starts to occur the instant that surface hydration drops below 100%.

From the indicator standards it is clear that there are two changes that occur when pH 5.6 thymol blue protonates. First, the peak height ratio of the peaks at 1240–1185 cm<sup>-1</sup> increases, and second, a peak in the region 1345 cm<sup>-1</sup> appears. The dry clay spectra show both of these changes, although it appears that there is a slight shift in the peak at 1345 cm<sup>-1</sup> to higher wavenumbers. In Fig. 4 individual spectra of the thymol blue are given before and after drying, together with the thymol blue species expected to be present on the clay surface.

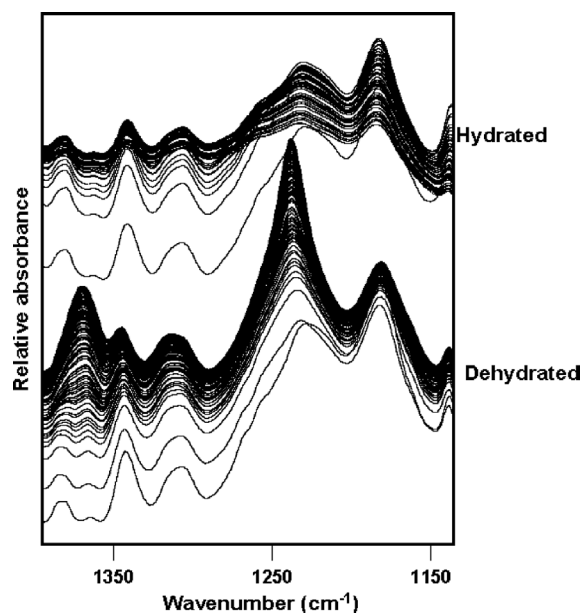


Fig. 3. Selected spectra for thymol blue sorbed onto a clay film allowed to air-dry over an 8-h period, during which a spectrum was collected every minute. Assignment of hydrated and dehydrated regions is based on changes in the water bands at 1600 cm<sup>-1</sup>.

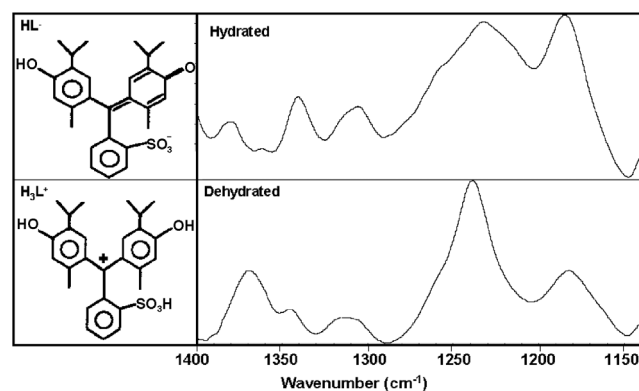


Fig. 4. Spectra of the sorbed thymol blue indicator on the hydrated and dehydrated surface together with the most likely thymol blue species present on the surface.

To illustrate the time frame over which the surface is dried and protonation begins, the peak height ratio of the peaks at 1240–1185 cm<sup>-1</sup> and the peak height of the peak at 1365 cm<sup>-1</sup> were plotted against time (Fig. 5). This figure clearly illustrates the rapid change that occurs when the surface begins to dry. It would appear that the changes in the sulfonate and phenolic groups occur simultaneously and that there is a critical water content at which protonation begins. Determination of this threshold could not be made accurately due to the extreme sensitivity required for low water content. Accurate measurement of surface water content would add great value to the technique. The current data nevertheless provide valuable spectroscopic evidence for the acidifying effect of drying and illustrate how radically and rapidly surface conditions change in response to changes in hydration state.

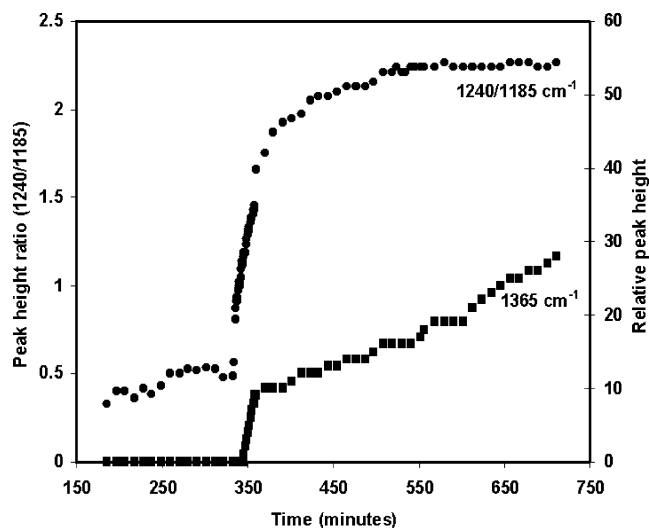


Fig. 5. Peak height ratio at 1240–1185  $\text{cm}^{-1}$  peaks (●) and peak height of the 1365  $\text{cm}^{-1}$  peak (■) as a function of time.

This acidifying effect has important implications for the surface chemistry of any solid–solution interface where the bathing solution has an appreciable ionic strength. A drying-induced pH change on a reactive surface is bound to have a profound influence on chemical interactions. For example, the generation of surface charge on amphiprotic surfaces is pH-dependent and a change in charge characteristics will influence the affinity of specific sorbates for the surface. Additionally, surface bound groups may also show speciation changes in accordance with the pH shift. Surface dissolution can also be a pH-mediated process. Proton- and ligand-promoted dissolution [13] of mineral surfaces are well recognized mechanisms of metal release, both of which involve surface protonation. The role of pH is fundamental in redox reactions, where lowering the pH significantly lowers the redox potential required to initiate reduction. This may explain the release of redox-sensitive Mn from dried soils and may play a role in the passivation of iron corrosion, which is known to be pH-dependent [8] toward the final stages of surface drying.

These results have demonstrated the clarity and ease with which the chemistry of a drying surface can be probed us-

ing the ATR technique. This technique opens opportunities in many branches of surface science for studying the critical period of dramatic change accompanying water loss from a surface. The simple demonstration of substantial pH change associated with drying points to the possible operation of other chemical thresholds, which could explain some of the anomalies reported in many branches of surface science. In terrestrial geochemistry most of our understanding comes from mineral–water investigations in fully hydrated systems. However, the spectroscopic evidence for the occurrence of these chemical transitions at ambient temperatures suggests a new paradigm for interpreting the changes that take place with moisture fluctuations at the solid–water interface.

### Acknowledgments

Financial support was provided by a graduate scholarship from the Skye Foundation and by the National Research Foundation of South Africa (Grant No. 2047381) and the Eskom Tertiary Education Support Programme.

### References

- [1] M.M. Mortland, K.V. Raman, *Clays Clay Miner.* 16 (1968) 393.
- [2] H.F. Birch, *Plant Soil.* 10 (1958) 9–31.
- [3] R.J. Bartlett, B.R. James, *Soil Sci. Soc. Am. J.* 44 (1980) 721.
- [4] R.J. Bartlett, B.R. James, *J. Environ. Qual.* 8 (1979) 31.
- [5] D.S. Ross, H.C. Hales, G.C. Shea-McCarthy, A. Lanzirotti, *Soil Sci. Soc. Am. J.* 65 (2001) 736.
- [6] A. Rahev, Y. Avnimelech, *Plant Soil* 50 (1978) 545.
- [7] C. Kennedy, D.S. Smith, L.A. Warren, *Geochim. Cosmochim. Acta* 68 (2004) 443.
- [8] A. Cox, S.B. Lyon, *Corros. Sci.* 36 (1994) 1177.
- [9] M.J. Borda, D.R. Strongin, M.A. Schoonen, *Spectrochim. Acta* 59 (2003) 1103.
- [10] O.W. Duckworth, S.T. Martin, *Geochim. Cosmochim. Acta* 65 (2001) 4289.
- [11] I.M. Kolthoff, M.K. Chantooni Jr., S. Bhowmik, *Anal. Chem.* 39 (1967) 315.
- [12] P. Balderas-Hernandez, M.T. Ramirez, A. Rojas-Hernandez, A. Gutierrez, *Talanta* 46 (1998) 1439.
- [13] B. Zinder, G. Furrer, W. Stumm, *Geochim. Cosmochim. Acta* 50 (1986) 1861.